Journal of Alloys and Compounds 494 (2010) 78–83

Contents lists available at ScienceDirect

Journal of Alloys and Compounds

journal homepage: www.elsevier.com/locate/jallcom

Impact of high pressure torsion on the microstructure and physical properties of $Pr_{0.67}Fe_3CoSb_{12}$, $Pr_{0.71}Fe_{3.5}Ni_{0.5}Sb_{12}$, and $Ba_{0.06}Co_4Sb_{12}$

L. Zhang[a,c], A. Grytsiv[a], B. Bonarski[c], M. Kerber[c], D. Setman[c], E. Schafler[c], P. Rogl[a,*], E. Bauer[b], G. Hilscher[b], M. Zehetbauer[c]

[a] Institute of Physical Chemistry, University of Vienna, Währingerstr. 42, A-1090 Vienna, Austria
[b] Institute of Solid State Physics, Vienna University of Technology, Wiedner Hauptstr. 8-10, A-1040 Vienna, Austria
[c] Research Group Physics of Nanostructured Materials, University of Vienna, Boltzmanngasse 5, A-1090 Vienna, Austria

ARTICLE INFO

Article history:
Received 11 December 2009
Accepted 9 January 2010
Available online 20 January 2010

Keywords:
Skutterudite
Severe plastic deformation
Nanomaterials
Thermoelectricity

ABSTRACT

Both p- and n-type skutterudites ($Pr_{0.67}Fe_3CoSb_{12}$, $Pr_{0.71}Fe_{3.5}Ni_{0.5}Sb_{12}$ and $Ba_{0.06}Co_4Sb_{12}$) have been deformed by high pressure torsion (HPT) with 2 GPa resulting in a lamellar shaped nanograined structure. The crystallite size distribution and dislocation density are evaluated using X-ray powder diffraction data, revealing a crystallite size of 47 nm and a dislocation density of 7×10^{14} m^{-2} for $Ba_{0.06}Co_4Sb_{12}$. Whilst at $T < 5.6$ K the electrical resistivities of HPT processed $Pr_{0.67}Fe_3CoSb_{12}$ and $Pr_{0.71}Fe_{3.5}Ni_{0.5}Sb_{12}$ do not indicate long-range magnetic order, the temperature dependent susceptibility elucidates antiferromagnetic ordering after HPT although the anomaly at the phase transition becomes washed out. The effective magnetic moments are 4.18μ_B and 4.07μ_B for $Pr_{0.67}Fe_3CoSb_{12}$ before and after HPT, revealing a non-zero effective moment on the Fe_3CoSb_{12} framework. Metamagnetic transitions at $\mu_0 H = 0.9$ (before HPT) and 0.8 (after HPT) are clearly seen in isothermal magnetization curves. In comparison with the microstructures of milled and hot pressed samples, those after HPT exhibit markedly smaller although lamellar grains, and also amorphous aggregates. The thermal conductivity of HPT samples is smaller, but the electrical resistivity is markedly higher than that of milled material, which in sum results in a lower figure of merit ZT. The increase of resistivity is caused by the high density of microcracks observed in the HPT samples, which may be avoided by suitable modification of the HPT processing parameters.

1. Introduction

Filled skutterudites, $R_yT_4Pn_{12}$ (R is a rare-earth or alkaline earth, T is a transition metal, Pn can be Sb, P or As), become one of the most prospective thermoelectric materials due to their intrinsic semiconducting behaviour and since the "Phonon Glass-Electron Crystal" concept [1] predicted a reduction in heat conduction via phonon scattering by atoms rattling in the cages of the skutterudite structure. TE properties are defined by the dimensionless figure of merit $ZT = (S^2/(\rho \cdot \kappa))T$, where S means the Seebeck coefficient, ρ the electrical resistivity, and κ the thermal conductivity. The thermal conductivity contains two parts: the electronic contribution (κ_e) and the phononic contribution (lattice thermal conductivity κ_l). It has been shown that a smaller grain size results in lower thermal conductivity [2] due to enhanced phonon boundary scattering at interfaces and crystal imperfections like dislocations. In addition, during heat treatment, small grains lead to higher densification. Therefore, there are numerous reports on ball milled and hot pressed (BM + HP) unfilled [3–8] and filled [9–13] skutterudites.

Mechanical milling is an appropriate method to produce nanograined powders, however an additional high temperature compacting step is necessary to form bulk materials. Besides that, there are some state-of-art deformation methods producing nanostructured materials from bulk to bulk directly. For $Ce_{0.29}Fe_{1.4}Co_{2.6}Sb_{11.24}$ uniaxial compression has been used under 150 MPa up to 20 cycles [14], for $CoSb_3$ high pressure sintering at 723 K in a pressure range from 2 to 6 GPa [15], and for $Co_4Sb_{12-x}Te_x$ also high pressure sintering at 900 K under 1.5 GPa [16]. Recently, however, the new methods of severe plastic deformation have been applied, also for preparation of thermoelectric materials, for instance, equal channel angular extrusion (ECAE) [17–21] and high pressure torsion (HPT) [22,23] for preparation of bismuth telluride based compounds. High Pressure Torsion (HPT), one of the most important techniques of severe plastic deformation (SPD), is capable of producing ultrafine-grained bulk materials [24–28]. During HPT, the specimen is subjected to a torsional strain under high

* Corresponding author at: Institute of Physical Chemistry, University of Vienna, Währingerstr. 42, A-1090 Vienna, Austria. Tel.: +43 1427752456; fax: +43 1427795245.
E-mail address: peter.franz.rogl@univie.ac.at (P. Rogl).

0925-8388/$ – see front matter © 2010 Elsevier B.V. All rights reserved.
doi:10.1016/j.jallcom.2010.01.042

hydrostatic pressure. In order to prevent the loaded material to flow out under high pressure, cavities are normally made in each of the two anvil supports.

To our knowledge, there is yet no investigation of the influence of HPT processing on skutterudites. In the present study, Pr-filled p-type $Pr_{0.67}Fe_3CoSb_{12}$ and $Pr_{0.71}Fe_{3.5}Ni_{0.5}Sb_{12}$, as well as Ba-filled n-type $Ba_{0.06}Co_4Sb_{12}$ were subjected to HPT grain refining. Grain size and defects were analysed by X-ray powder diffraction (XPD) and scanning electron microscopy (SEM), and thermoelectric as well as magnetic properties were investigated.

2. Experimental procedures

Samples were prepared in an amount of 10 g each. $Ba_{0.06}Co_4Sb_{12}$ was prepared from pieces of Ba (99+ mass%, Sigma–Aldrich, Germany) Co powder (99.9 mass%, particle size <150 μm, Sigma–Aldrich, Germany) and Sb ingot (99.9 mass% metals basis, Alfa Aesar, Germany); $Pr_{0.67}Fe_3CoSb_{12}$ and $Pr_{0.71}Fe_{3.5}Ni_{0.5}Sb_{12}$ were prepared from pieces of Pr (99.9 mass%, Rhône-Poulenc, Shelton, CT), wire of Fe and Ni (each of purity of 99.9 mass%, from Alfa Aesar, Germany), and Sb ingot (99.9 mass% metals basis, Alfa Aesar, Germany). The processes for synthesis can be found in our previous papers [8,13,29]. The precursors were milled by hand to powder, loaded in a 10 mm diameter graphite die inside a glove box and were hot pressed under Ar atmosphere in an FCT hot-press system HP W 200/250 2200-200-KS at 600 °C under 56 MPa during 2 h. The hot pressed samples were cut to disks and enclosed in a Cu ring to improve the deformation behaviour during HPT as in [30]. The samples were deformed using HPT at room temperature, in air and at a pressure of 2 GPa for one revolution.

X-ray powder diffraction data were obtained from a HUBER Guinier powder camera and monochromatic Cu $K_{\alpha1}$ radiation ($\lambda = 0.154051$ nm) with an image plate recording system. Precise lattice parameters were calculated by least squares fits to the indexed 2θ values using Ge as internal standard ($a_{Ge} = 0.565791$ nm). The filling fraction, y, was calculated from Rietveld refinements employing the program FULLPROF [31].

The crystallite size distribution for coherent-scattering-domains (CSD) was evaluated from the Convolution Multiple Whole Profile (CMWP) fitting [32,33] with proper instrumental correction, which allows to determine also the absolute value of dislocation density. Instrumental broadening of the diffraction maxima is accounted for by using an internal standard (Si), defining the instrument independent FWHM (β). For a detailed description of the crystallite size evaluation, see [8]. Images of the fracture surfaces were taken with a Philips XL30 field emission environmental scanning electron microscope (ESEM-FEG).

The low temperature ($4 < T < 300$ K) electrical resistivity was measured using a four-probe dc method; measurements of the Seebeck coefficient were carried out with a differential method in a home-made apparatus. The measurements of the high temperature Seebeck coefficient ($300 < T < 800$ K) and electrical resistivity were performed using a ZEM-3 system (Ulvac-Riko, Japan). The thermal conductivity was calculated from the thermal diffusivity D_t, specific heat C_p and density ρ_d, measured by a laser flash method (Flashline-3000, ANTER, USA), using the relationship $\kappa = D_t C_p \rho_d$. The density of the samples before HPT was obtained by the Archimedes' method using distilled water, whereas the direct volume method was used for the samples after HPT, because the density of microcracks was too high to employ Archimedes' method. Our previous data prove that the two methods are in good agreement with each other [13].

The lattice thermal conductivity κ_l was calculated by subtracting the electronic thermal conductivity κ_e (employing the Wiedemann–Franz law and assuming a temperature independent Lorenz number $L_0 = 2.44 \times 10^{-8}\ V^2/K^2$) from the measured κ. A superconducting quantum interference device (SQUID) was employed for the determination of the magnetization from 3 K up to 300 K in fields up to 3 T for $Pr_{0.67}Fe_3CoSb_{12}$ before and after HPT with the weight of pieces being 81.16 and 30.54 mg, respectively.

3. Results and discussion

3.1. X-ray powder diffraction analysis and evaluation of crystallite size

The Rietveld refinement data evaluated from XPD show the same Pr filling fractions before and after HPT (Table 1). However, the lattice parameters for all three samples seem to become larger after HPT (Table 1). The relative changes $\Delta a/a$ for $Ba_{0.06}Co_4Sb_{12}$, $Pr_{0.67}Fe_3CoSb_{12}$ and $Pr_{0.71}Fe_{3.5}Ni_{0.5}Sb_{12}$ amount to 1.6×10^{-4}, 6.2×10^{-4} and 6.3×10^{-4}, respectively. Comparing the XPD profiles (Fig. 1) for $Pr_{0.67}Fe_3CoSb_{12}$ before and after HPT, peak broadening is clearly observed after HPT.

Table 1
Room temperature lattice parameter (a), and relative density (den.) for skutterudites before HPT (NOR) and after HPT (HPT). CSD size was calculated by using CMWP (see text).

Composition	Preparation method	a (nm)	Den. (%)	CSD size (nm)
$Ba_{0.06}Co_4Sb_{12}$	NOR	0.90395(3)	98.1	
$Ba_{0.06}Co_4Sb_{12}$	HPT	0.90409(1)	91.4	47
$Pr_{0.67}Fe_3CoSb_{12}$	NOR	0.91111(2)	95.5	
$Pr_{0.67}Fe_3CoSb_{12}$	HPT	0.91167(5)	78.4	
$Pr_{0.71}Fe_{3.5}Ni_{0.5}Sb_{12}$	NOR	0.91209(4)	96.7	
$Pr_{0.71}Fe_{3.5}Ni_{0.5}Sb_{12}$	HPT	0.91266(5)	83.5	

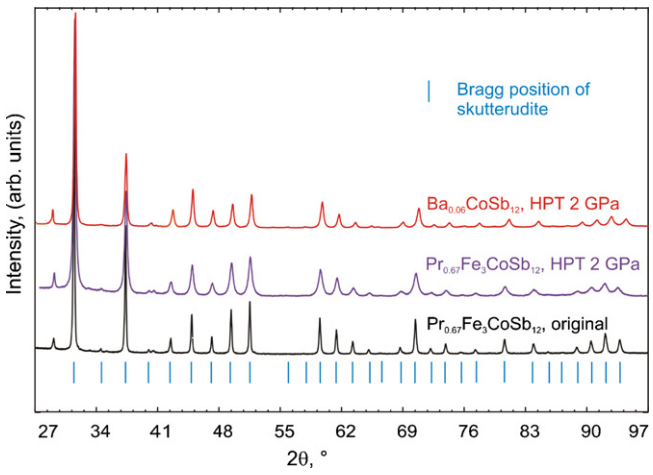

Fig. 1. Selected XPD patterns evidencing the skutterudite structure for the unperturbed samples and the material achieved by HPT at 2 GPa.

Fig. 2 gives the crystallite size distribution for HPT $Ba_{0.06}Co_4Sb_{12}$ in comparison with BM + HP (ball milled and hot pressed) $CoSb_3$ [8] and BM + HP $Mm_{0.85}Fe_4Sb_{12}$ with 2.7 wt.% Mm_2O_3 in situ precipitation [13]. The crystallite size distributions for HPT $Ba_{0.06}Co_4Sb_{12}$ were evaluated from CMWP for both ellipsoidal and spherical grain shape, respectively. The standard errors from the former are much lower than from the latter, and an ellipticity of CSD, $\varepsilon_e = 4.8$, results from CMWP which roughly corresponds to the anisotropy of lamella size reported in Fig. 3. Since the differences of R (Ba, Mm) and T (Co or Fe) for $R_yT_4Sb_{12}$ do not affect the crystallite size, we can compare the crystallite sizes resulting from HPT $Ba_{0.06}Co_4Sb_{12}$ sam-

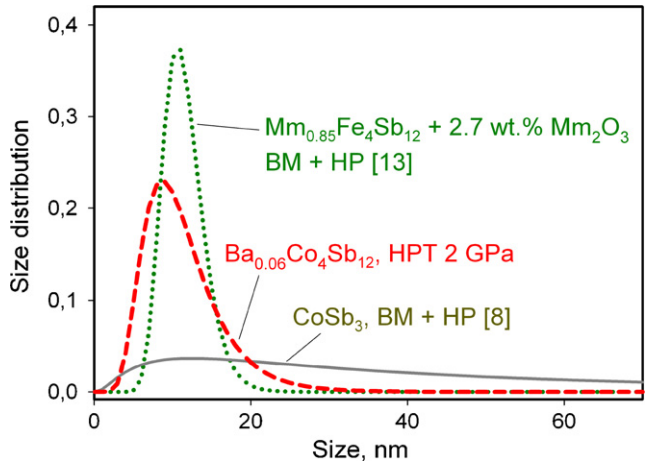

Fig. 2. Crystallite size distributions for HPT samples processed at 2 GPa, in comparison to ball milled and hot pressed (BM + HP) specimens [8,13].